

McKenzie Gorman, Thomas Pham, Lauren Nenow

Professor Weingarten

GEOL 600

11 May 2025

Deep Water Horizon Blow Out Simulation

On April 20th, 2010, approximately 41 miles off the coast of Louisiana, one of the most catastrophic environmental disasters in US history unfolded. The failure of multiple safety systems at the Macondo Well led to a sudden surge of hydrocarbons being released under extreme pressure. The resulting explosion killed 11 workers, sank the Deepwater Horizon rig two days later, and triggered an uncontrolled oil spill from the seafloor. The blowout continued for 86 days before containment began with a “well integrity test”, but the well was not declared dead until September 19th, 2010 (Hsieh, 2011). The well integrity test consisted of six “valve turns, separated by 10-min rest periods” while pressures within the reservoir were monitored, to determine the likelihood of leakage from the well into the surrounding formation (Hsieh, 2011). If the pressure was greater than 7500 psi, the risk of leakage was low, and it was safe to permanently seal the well. If the shut-in pressure was less than 6000 psi, the risk of leakage was high, and the well should be reopened to avoid irreparable damage to the surrounding rock. Finally, if the pressure was between 6000 and 7500 psi, the risk of leakage was unknown and the test should proceed for 24 hours. In the afternoon on July 15th, the well integrity test was performed and pressures settled within the unknown risk range. Data was then sent to Hsieh to model potential outcomes of shutting the well permanently.

This environmental disaster not only exposed regulatory, technical, and safety vulnerabilities in offshore drilling, but also prompted a reevaluation of industry standards and the

implementation of more stringent preventative measures. In response, our objective was to develop a groundwater flow model to estimate the total volume of oil spilled and understand the reservoir behavior during the well integrity test and following the capping of the well. Using USGS Modflow-2005, we constructed a detailed hydrologic model of the Macondo reservoir and well, simulated pressure responses, calibrated parameters, and compared our results to published spill volume estimates.

The Macondo Well is located at $28^{\circ}44'12''$ N and $88^{\circ}23'14''$ W within the modern Mississippi submarine canyon channel system. The top of the Macondo reservoir, in which the well was drilled, sits at approximately 18,000 ft below sea level and consists of three sand layers with a total thickness of 90ft. It is overlain by 13,000ft of sandstone interbedded with shales, siltstones and mudstones and BP's Deepwater Horizon accident report dates the reservoir to the Miocene epoch. To hopefully gain some insight into the geology of the reservoir we looked at a study done by Posamentier in 2003 on the Pleistocene aged Desoto Canyon submarine channel

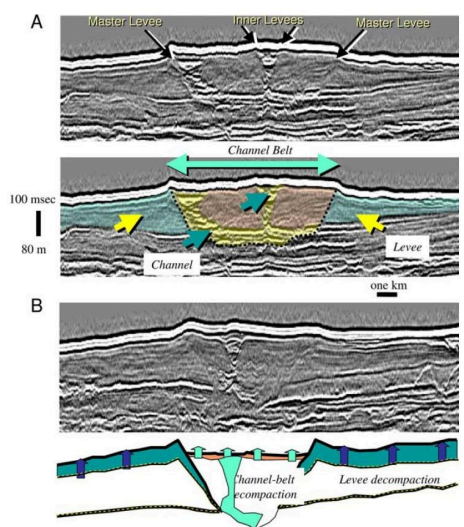


Fig. 12. (A) Transverse seismic reflection profile across the Joshua channel belt and associated levees. The master bounding levees as well as the levees bounding the Joshua channel are shown. The channel is inferred to be most sand prone, followed by the channel belt, which is less sand prone, and the overbank, which is least sand prone. (B) illustrates the decompacted configuration of the leveed channel system.

Figure 12 (Posamentier, 2011)

system. We know that the general geology trends of the Northern Gulf of Mexico include many submarine channel systems and that the Desoto System is situated in the northeastern area of the gulf. We learn that the channels of the DeSoto system are described as “differentially compacted” and deposited via multiple turbidity flows (Posamentier, 2003). The initial flow formed the levees of the channel from silty, easy to compact sands. This was then followed by a flow of coarser, harder to compact sands that accumulated and filled the channel itself. Transverse

seismic reflection profiles done across the Joshua channel belt revealed that multiple channels were formed this way, in close proximity to one another, and within yet another set of larger levees. These “master-bounding levees” encompass multiple smaller, more sinuous channels, resulting in a larger and much more linear channel (Fig. 12, Posamentier, 2003).

Despite the age difference of at least 2.7 million years between the Macondo reservoir and the DeSoto Canyon, we can safely assume the geological processes associated with their formation are the same due to the overall geology of the Northern Gulf of Mexico being dominated by submarine channel systems. We can also assume the multiple sand layers of the Macondo reservoir are individual channels within a set of master-bounding levees like those of the Desoto canyon belt. The silty sands of the master-bounding levees form the aquitard, enclosing the multiple channels of coarser reservoir sands and creating a pressurized system

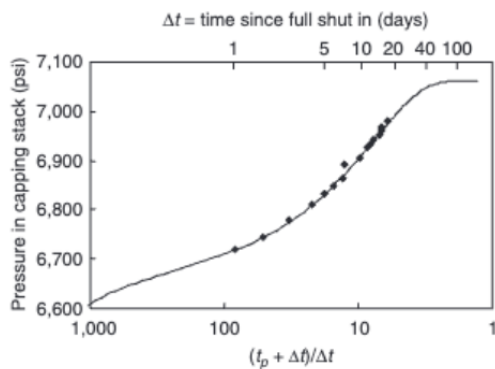


Figure 1: Horner Plot (Hsieh, 2011)

ideal for oil extraction. The Macondo reservoir had a high initial pressure, which was nothing abnormal for sediments of the area. Hsieh used a Horner plot to analyze ongoing shut-in pressure data from the well to further refine his model (Figure 1, Hsieh, 2011). This also supported the idea that the reservoir geometry was

elongated rather than square, reinforcing the channel-based formation theory. With this background knowledge on the hydrogeology of the area, we moved forward with the construction of our model in MODFLOW.

Our first step was creating the domain of our reservoir and incorporating the given parameters as well as our assumptions. Our model domain spans an area of 4,000ft in the x direction and 1,500 ft in the y direction with a depth of 90 ft in the z direction. Our well was

placed within the cell located 300 ft in the x direction and 400 ft in the y direction. Beginning at the well, the grid uses an initial cell size of 0.8 ft by 0.8 ft. Through discretization, the cell size increases away from the well by 20 percent until a size of 5 ft by 5 ft is reached. Once the 5 ft cell size is achieved, it is maintained consistently throughout the remainder of the model domain. We applied no flow boundaries at the borders of the model, and used given aquifer property ranges for hydraulic conductivity and specific storage. Additionally, we built an observation well with head values for key time points, most important of which was day 86, and the hour following, as the closure of the well and the well integrity test began (Figure 1, Pham, Gorman, Nenow). At day 86, the pumping rate was approximately 280,000 ft³/day. The closure process involved incrementally closing a valve within the well. Each time the valve was turned towards closure, the pumping rate decreased by approximately 40,000 ft³/day (Fig. 3, Hsieh, 2011). The well flowed at this decreased rate for 10 minutes during a waiting period before the next turn occurred. The process of closing the well included 6 valve turns across a period of 1 hour, after which the pumping rate reached 0 ft³. We see in Figure 3 from Hsieh that the pressures within the well stabilize after this point. The given head values also reflect this stabilization as the aquifer begins to recover towards equilibrium (Figure 2, Pham, Gorman, Nenow).

WEL: Well package				
Formula				
Starting time	Ending time	Pumping rate	Well Multiplier	
PEST Modifier		none	none	
Modification Method		Multiply	Multiply	
0	86	-280729	1	
86	86.00694	-240624.9	1	
86.00694	86.01389	-200520.7	1	
86.01389	86.02083	-160416.6	1	
86.02083	86.02778	-120312.4	1	
86.02778	86.03472	-80208.29	1	
86.03472	86.04167	-40104.14	1	
86.04167	120	0	1	

Figure 1: MODFLOW Well Package (Pham, Gorman, Nenow)

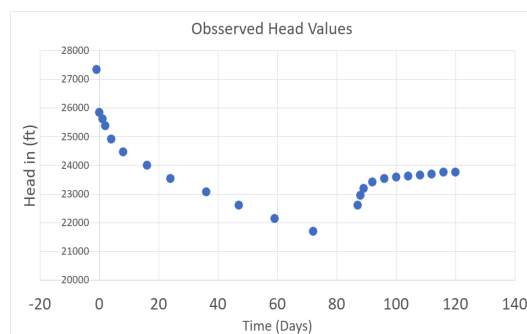


Figure 2: Observed Reservoir Pressure at Well (Pham, Gorman, Nenow)

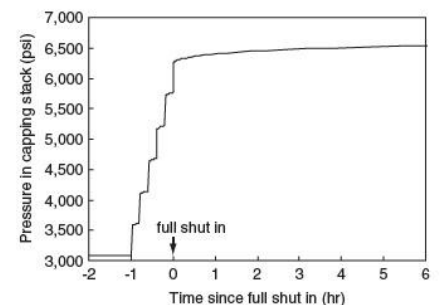


Figure 3. Simulated pressure in the capping stack of the Macondo well. Start of the shut-in process occurs at time = -1 h. Full shut in occurs at time = 0 h. The line shows the simulated pressure calculated by the initial model. The simulated pressure closely matched the observed pressure data, which are not shown due to their proprietary nature.

Figure 3, (Hsieh, 2011)

To constrain our model, we applied various assumptions based on standards for pressure and flow analysis in oil wells. These included the reservoir being horizontal, the fluid compressibility being small and constant (similar to water), and that small enough pressure gradients existed for Darcy's law to apply. Referencing the equation for oil flow in a reservoir, we also assumed that:

- The flow of oil was under liquid and isothermal conditions
- The permeability, porosity, and compressibility were homogeneous
- Permeability and viscosity are independent of pressure
- Permeability is isotropic

Some of our own assumptions included radial flow of oil, that the reservoir is homogeneous in the x and y direction, and that the vertical conductivity is 1/10th of the horizontal conductivity. With these assumptions applied to our model domain and parameters, we moved on to calibration of our model in order to obtain the most accurate results with our limited information.

Our initial guesses for conductivity and specific storage of the reservoir produced high residuals in the hundreds of thousands. However, through iterative calibration, we observed the behaviors of both hydraulic conductivity and specific storage. Increasing conductivity raised the head values and thus improved head rebound rates. Increasing specific storage also contributed to raising the total available head by increasing the amount of oil available for pumping. Additionally, we found that reducing specific storage flattened the head gradient in the final stress period while alternatively, decreasing hydraulic conductivity and increasing specific storage steepened the gradient. By analyzing the results of numerous model runs, we concluded that the model has more sensitivity to changes in specific storage towards the end of the graph, after the well is closed, while conductivity has a greater effect at the beginning of the graph,

before the closure process begins. This is because the flow rate is the most dominant controlling factor of the head values while the well is actively pumping, whereas the specific storage is the most dominant controlling factor as the aquifer is recovering and the head gradients are flattening.

In order to determine the accuracy of our chosen hydraulic conductivity and specific storage values, we plotted the variables against the RMS error. To better visualize the effects of

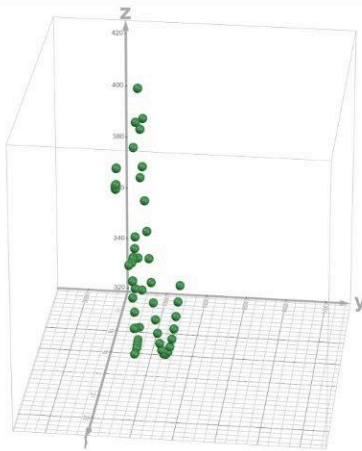


Figure 3: K & SS vs. RMS in Desmos (Pham, Gorman, Nenow)

changes to the hydraulic conductivity and specific storage on the RMS value, we created a 3-dimensional graph in Desmos (Figure 3, Pham, Gorman, Nenow). We were able to identify a local minimum in our RMS value through our 3-dimensional visualization, and the associated ranges in specific storage and conductivity values. We saw that deviation from these ranges of specific storage and conductivity resulted in immediate, steep rises in the RMS calculation. Our best-fit model achieved our lowest RMS of 319.885 and an absolute residual sum of 1,178.172 ft. Our most accurate hydraulic conductivity value was 1.925 ft/day and our specific storage value was 1.275×10^{-5}

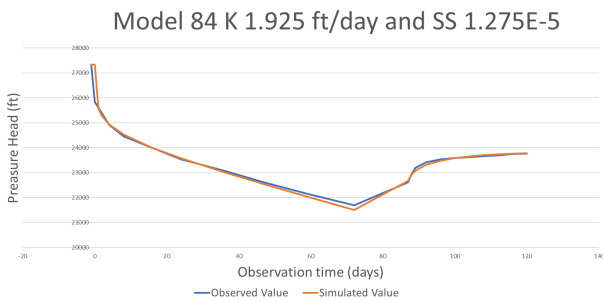


Figure 4: Best-fit Model (Pham, Gorman, Nenow)

(Figure 4, Pham, Gorman, Nenow).

Once we had an accurate, calibrated model, it became clear that the flow pattern was linear instead of radial, a realization that emerged while observing the change in the head gradient and response curve after the pumping rate dropped to $0 \text{ ft}^3/\text{day}$. We decided to reposition the observation well along the same strike as the pumping well and rotate the grid to bring the

well closer to the domain boundary, where head changes were more sensitive. This helped sharpen the simulated response and reduce the RMS. After calibrating our best-fit model, we were able to analyze our results and see how they compared to others in the scientific community.

After the well was closed, our model showed a head gradient gently sloping from right to left towards the well, with a slope of 0.027525. This gentle slope indicated stable pressures across the domain and showed that the reservoir was not likely to leak into the surrounding rock. If the slope was steeper, or reversed in direction, our model would show the reservoir at risk for elevated stress conditions and an increased risk of leakage. Notably, both the lower and upper bound head gradients were above 23,000 ft, which was well above the 13,000 ft threshold (6,000 PSI). Based on the modeled pressure heads and gradient at day 119, the reservoir appears secure with no indication of potential leakage.

Once we knew the reservoir was stable, we moved on to estimate the total oil spilled during the Deepwater Horizon disaster. We assumed a constant spill rate of 280,729 ft³/day for the first 86 days, followed by a series of decreasing flow rates over six 10-minute steps as the well was incrementally closed. After performing a summation of volumes in Excel, our total spill estimate was 24,148,542.52 ft³ or roughly 4.3 million barrels of oil. A study published by the National Academy of Sciences in 2011 compared different theories on breach points in the Macondo well and their associated spill volumes. The average spill volume calculated by the

Period Multiplier	Pumping rate	Turn steps	Time (days)	Volume of oil (ft ³)
86	280729		86	24142694
1	240624.86	1	0.00694	1671.01
2	200520.71	2	0.00694	1392.5
3	160416.57	3	0.00694	1114
4	120312.43	4	0.00694	835.5
5	80208.29	5	0.00694	557
6	40104.14	6	0.00694	278.5
17	0		17	0
Total				24148542.51

teams involved was 26,591,808.16 ft³ or

approximately 4.7 million barrels of oil (McNutt et al., 2011). Our estimate falls short by about

435,164 barrels, resulting in a 9.19%

Figure 5: Spill Calculations (Pham, Gorman, Nenow)

underestimation. The difference likely stems from our modeling approach. We began with a lower starting pumping rate than was likely accurate and we did not simulate a gradually decreasing flow over the first 86 days. Due to these factors, while we cannot determine the exact volume of oil spilled, our model was still able to give a conservative estimate that aligned reasonably well with publicly available sources, given the limited data available to us.

Even though our model indicated a reasonable estimate, it is important to acknowledge that all models have their limitations. One of the most significant constraints on our model was the small dataset provided of only 23 observed head values. This limited number of data points made it difficult to determine the model's accuracy with high confidence. In comparison Hsieh was able to improve the accuracy of his model after the shut-in process as more data became available, allowing for better calibration and refinement (Hsieh, 2011). Another important limitation is the lack of spatial data related to the position of the Macondo Well relative to the reservoir's no-flow boundaries, as well as the reservoir's total area and volume. These unknown characteristics made it harder to constrain the model and initially prevented us from accurately simulating head gradients within the system. Despite these limitations, our model demonstrated several notable strengths. The Root Mean Square (RMS) error of 319.885 indicates a relatively

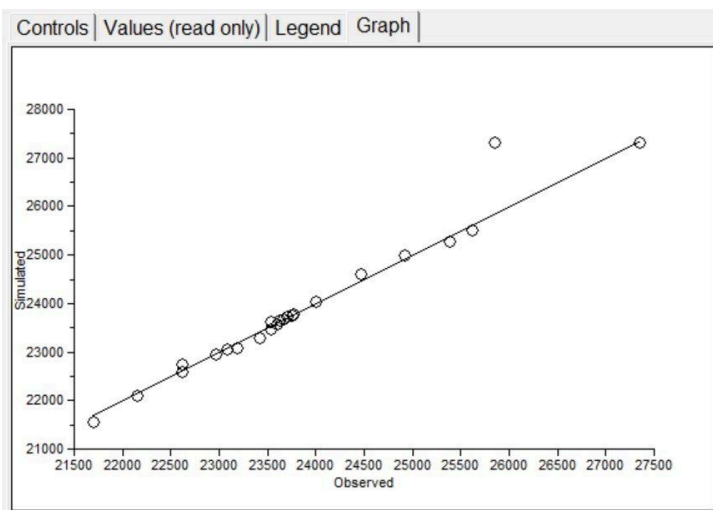


Figure 6: Absolute Value Residual Sum Graph (Pham, Gorman, Nenow)

strong fit between observed and simulated values given the available data. Through iteratively adjusting hydraulic conductivity, specific storage, and repositioning the observation well, we were able to minimize this error and arrive at the most accurate model

possible. Additionally, the Absolute Value Residual Sum of 1,178.172 ft further supports the overall reliability of our model (Figure 6, Pham, Gorman, Nenow). We would like to note that this value excludes the far-right outlier shown in Figure 6, which was omitted due to a lack of supporting data before the shut-in procedure began. The plot in Figure 6 also reinforces our model's fit, with simulated data points closely aligned along the observed trend. The simulated values are evenly distributed above and below the observed values trend line, indicating balanced deviations. Finally, a key strength of our model is its flexibility and adaptability. It can be updated with future data inputs, or repurposed for the simulation of other blowout scenarios. These characteristics make it a valuable tool for analyzing similar events, even when operating under data-limited conditions.

Following the closure of the Macondo Well, there were several immediate actions taken by BP to ensure the permanent closure of the well and implementation of the "oil spill response (OSR)" (Offshore Technology, 2010). A "static kill" operation was initiated, which involved injecting heavy drilling mud and cement into the well to seal it (BP, 2010). A relief well was also drilled to intercept the Macondo well and ensure complete isolation of the reservoir. Efforts directed towards environmental recovery included site remediation via "spill response vessels including skimmers, tugs, barges, and recovery vessels" (Offshore Technology, 2010) to collect oil from the surface ocean. Oil dispersant was also used and deployed via aircraft.

For approximately 2 years after the blowout, there was continuous monitoring of the well by Transocean and BP via remotely operated vehicles (Offshore Technology, 2010). However, based on the scale of this disaster, we think that monitoring should have been continued to ensure there were no signs of subsidence, unnatural seepage, or shifting of sediments around the well on the ocean floor. These movements could indicate underlying pressure changes or instability,

which could lead to future pressure build-up and leaks. The extent and duration of this disaster suggests a longer period of monitoring would have been appropriate to fully ensure long-term safety. According to the Department of the Interior, who studied the likely causes of the blowout, if we continue to do offshore drilling, there needs to be substantial reforms to the current practice, including double barrier systems, mandatory real-time monitoring of all aspects of the well, required stronger casing, cementing, and pressure management protocols (US Department of the Interior & BOEMRE, 2011).

In conclusion, our group was able to build, calibrate, and run a successful and very technical MODFLOW model in order to estimate the total amount of oil released from the Macondo Well from the blowout on April 20th. Although our final estimate of approximately 4.3 million barrels of spilled oil was slightly lower than what we would expect, it still aligns closely with other estimates given limited data availability and modeling assumptions. Looking ahead, this project reinforces the importance of long-term monitoring and the implementation of mandatory safety procedures for offshore drilling. Our work not only offers a valuable analytical tool but also contributes to the broader conversation about responsible offshore energy practices.

References

- BP. “Deepwater Horizon Accident Investigation Report.” *Www.Bp.Com*, 8 Sept. 2010,
www.bp.com/content/dam/bp/business-sites/en/global/corporate/pdfs/sustainability/issue-briefings/deepwater-horizon-accident-investigation-report.pdf.
- Conti, A., et al. “Morpho-acoustic characterization of natural seepage features near the Macondo wellhead (ECOGIG Site OC26, Gulf of Mexico).” *Deep Sea Research Part II: Topical Studies in Oceanography*, vol. 129, July 2016, pp. 53–65, <https://doi.org/10.1016/j.dsr2.2015.11.011>.
- Det Norske Veritas. (2011). *Forensic examination of Deepwater Horizon blowout preventer*. JOIFF.
<https://www.joiff.com/members/sharedlearning/topics/archive2011/documents/DWHFINAL.pdf>
- “Gulf Oil Spill: Scientists Develop New Model for Deep-Water Oil Spills.” *U.S. National Science Foundation*, 20 Apr. 2012,
www.nsf.gov/news/gulf-oil-spill-scientists-develop-new-model-deep#image-caption-credit-block%20%E2%80%8B%20%E2%80%8B.
- Hickman, Stephen H., et al. “Scientific basis for safely shutting in the Macondo well after the April 20, 2010 Deepwater Horizon blowout.” *Proceedings of the National Academy of Sciences*, vol. 109, no. 50, 3 Dec. 2012, pp. 20268–20273, <https://doi.org/10.1073/pnas.1115847109>.
- Hsieh, Paul A. “Application of MODFLOW for oil reservoir simulation during the Deepwater Horizon Crisis.” *Ground Water*, vol. 49, no. 3, June 2011, pp. 319–323, <https://doi.org/10.1111/j.1745-6584.2011.00813.x>.
- McNutt, Marcia K., et al. “Review of flow rate estimates of the Deepwater Horizon oil spill.” *Proceedings of the National Academy of Sciences*, vol. 109, no. 50, 20 Dec. 2011, pp. 20260–20267,
<https://doi.org/10.1073/pnas.1112139108>.
- Posamentier, Henry W. “Depositional elements associated with a basin floor channel-levee system: Case study from the Gulf of Mexico.” *Marine and Petroleum Geology*, vol. 20, no. 6–8, 14 Jan. 2003, pp. 677–690,
<https://doi.org/10.1016/j.marpetgeo.2003.01.002>.
- U.S. Department of the Interior, & Bureau of Ocean Energy Management, Regulation and Enforcement. (2011).
Deepwater Horizon: Report of the Department of the Interior investigation.
<https://www.joiff.com/members/sharedlearning/topics/archive2011/documents/DWHFINAL.pdf>